

ATOMIC CARBON IN THE W 3 GIANT MOLECULAR CLOUD

TAKESHI SAKAI¹, TOMOHARU OKA², AND SATOSHI YAMAMOTO³

¹Nobeyama Radio Observatory, Minamimaki, Minamisaku Nagano, 384-1305, Japan

E-mail: sakai@nro.nao.ac.jp

²Department of Physics, The University of Tokyo, 7-3-1, Hongo, Bunkyo-ku, Tokyo 113-0033, Japan

E-mail: tomo@taurus.phys.s.u-tokyo.ac.jp

³Department of Physics, The University of Tokyo, 7-3-1, Hongo, Bunkyo-ku, Tokyo 113-0033, Japan

E-mail: yamamoto@phys.s.u-tokyo.ac.jp

(Received February 1, 2005; Accepted March 15, 2005)

ABSTRACT

We have mapped the W 3 giant molecular cloud in the $C^0 \ ^3P_1-^3P_0$ ([CI]) line with the Mount Fuji Submillimeter-wave Telescope. The [CI] emission is extended over the molecular cloud, having peaks at three star forming clouds; W 3(Main), W 3(OH), and AFGL 333. The [CI] emission is found to be strong in the AFGL 333 cloud. We have also observed the $C^{18}O$, CCS, N_2H^+ , and $H^{13}CO^+$ lines by using the Nobeyama Radio Observatory 45 m telescope. In the AFGL 333 cloud, we find two massive cores, which are highly gravitationally bound and have no sign of active star formation. The high $[C^0]/[CO]$ and $[CCS]/[N_2H^+]$ abundance ratios suggest that the AFGL 333 cloud is younger than the W 3(Main) and W 3(OH) clouds.

Key words : ISM: individual: W 3 — ISM: clouds — ISM: atoms — submillimeter [CI] lines

I. INTRODUCTION

The W3/W4 HII region complex is an active star-forming site located in the Perseus arm at a distance of 2.35 kpc from the Sun (Massey, Johnson & Eastwood, 1995). Lada et al. (1978) found that a giant molecular cloud (GMC) is associated with the W 3 HII region. They also found that the most recent OB star formation has occurred mainly in the eastern edge of the W 3 GMC, which is called the high density layer (HDL). Since the HDL is parallel to the ionization front of the W 4 giant HII region, they proposed that the materials in the HDL may have been swept up by the expansion of the W 4 giant HII region.

Lada et al. (1978) show that three bright CO condensations exist in the HDL; W 3(Main), W 3(OH), and AFGL 333. Although these three condensations are similar in size and mass, being situated under similar environment, they exhibit different star-forming activities. W 3(Main), which is the most active star-forming region in the W 3 GMC, contains more than ten OB stars (Tieftrunk et al. 1997, 1998 and references therein). In W 3(OH), there is an ultracompact (UC) HII region containing a B0.5 star (Carpenter et al. 2000). The infrared source, AFGL 333, is a compact HII region, which contain a B0.5 star (Hughes & Viner 1982). AFGL 333 is relatively quiescent as compared with W 3(Main) and W 3(OH), where the infrared luminosities in W 3(Main), W 3(OH) and AFGL 333 are in the ratio 1.0:0.25:0.07 (Thronson et al. 1980).

The submillimeter lines of atomic carbon, $C^0 \ ^3P_1-^3P_0$ ([CI] 492 GHz) and $C^0 \ ^3P_2-^3P_1$ ([CI] 809 GHz), may be promising tools to study the evolutionary stages of molecular clouds. Recent large scale [CI] mapping observations by our Mount Fuji submillimeter-wave telescope group have revealed that C^0 is widely extended to molecular clouds (Sakai et al. in this issue, and references therein). They suggest that C^0 exists in the deep inside of molecular cloud, unlike the ancient picture based on the steady-state PDR models (e.g. Tielens & Hollenbach, 1985), where C^0 exists only in a thin layer near the surface of a molecular cloud. It has been pointed out that the time dependent chemistry can explain an origin of C^0 deep inside of a molecular cloud, since C^0 is slowly converted to CO in the course of cloud evolution (Lee et al. 1996, Oka et al. 2004, Kuboi et al. 2005). Thus the abundance ratio of C^0 and CO can be used as a tracer of the age of molecular clouds.

In this paper, we report the results of the large scale $C^0 \ ^3P_1-^3P_0$ observations toward the W 3 GMC by using the Mount Fuji submillimeter-wave telescope, and high spatial resolution mapping observation in the $C^{18}O \ J=1-0$ line with the Nobeyama Radio Observatory 45 m telescope. We also observed the CCS, N_2H^+ , and $H^{13}CO^+$ lines toward several positions in the W 3 GMC.

II. OBSERVATION

(a) Mount Fuji Observations

We observed the $C^0 \ ^3P_1-^3P_0$ line (492.160651 GHz; Yamamoto & Saito, 1991) with the Mount Fuji sub

Proceedings of the 6th East Asian Meeting of Astronomy, held at Seoul National University, Korea, from October 18-22, 2004.

-millimeter-wave telescope. The diameter of the main reflector is 1.2 m, corresponding to the half power beam widths of $2'.2$ at 492 GHz. The observations were carried out during four observing seasons from 1998 to 2003. The large scale mapping observations of the $C^0\ ^3P_1-^3P_0$ line was carried out with a grid spacing of $3'$ (hereafter, coarse-grid) from 1998 to 2000, whereas the detailed mapping observations of the $C^0\ ^3P_1-^3P_0$ line in several bright regions were carried out with a grid spacing of $1'.5$ (hereafter, fine-grid) from 2001 to 2003. We used an acousto-optical spectrometer (AOS), whose band width and effective resolution are 900 MHz and 1.6 MHz, respectively.

The telescope pointing errors were corrected by observing the thermal continuum emission from the full moon and the sun at 492 GHz. The pointing observation was carried out every month. The pointing accuracy was kept to be better than $20''$ in r.m.s., and checked by observing the standard sources, Orion KL and M17 every observing day.

We employed the position switching mode for all observations. Antenna temperature was calibrated by the single load chopper wheel method. The main beam efficiency was estimated to be 0.45 for 492 GHz, respectively. For the coarse-grid map, the reproducibility of the intensity was within 15 % ($1\ \sigma$). For the fine-grid maps, the reproducibility was within 7 % ($1\ \sigma$). We use the fine-grid mapping [CI] data for quantitative analyses.

(b) NRO 45 m Telescope Observations

The $C^{18}O\ J=1-0$ line was observed with the BEARS 25-multi beam array installed on the Nobeyama Radio Observatory (NRO) 45 m telescope. The observations for the CO lines were carried out from March 8 to March 10 in 2002. The observing grid is $20''.55$. The backend was a digital auto-correlator in the high resolution mode, whose bandwidth and resolution are 32 MHz and 31.25 kHz, respectively. All the observations were performed with a position switching mode. The pointing accuracy was checked by observing the SiO maser source (S-Per) every 2 hours, and was maintained to $\leq 5''$. The line intensity was calibrated by a chopper wheel method. The intensity of each receiver channel of BEARS were scaled to the intensity observed with the S100 receiver toward the Orion KL region. Then the main beam temperature (T_{MB}) was determined by dividing the antenna temperature by the main beam efficiency for the S100 receiver.

The CCS $J_N=4_3-3_2$, $N_2H^+\ J=1-0$, and $H^{13}CO^+\ J=1-0$ lines were observed on March 13, 2001. We used the SIS receivers (S40 and S100) for observations in the 40 GHz and 80–110 GHz bands. The backend was the AOS-H, whose bandwidth and resolution are 40 MHz and 37 kHz, respectively. The pointing accuracy was maintained to $\leq 5''$.

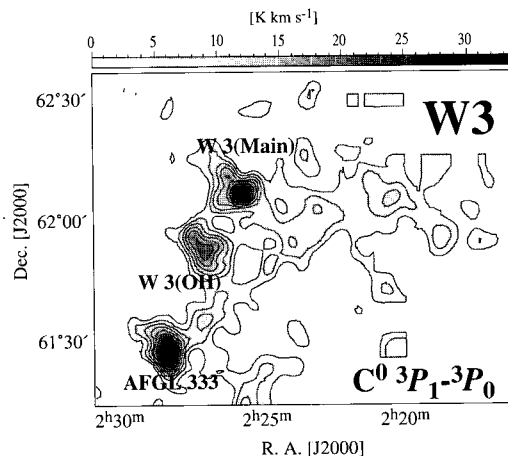


Fig. 1.— Integrated intensity map of the $C^0\ ^3P_1-^3P_0$ emission toward the W 3 GMC.

III. RESULTS

(a) [CI] Distribution

Fig. 1 shows the integrated intensity map of the $C^0\ ^3P_1-^3P_0$ line (hereafter, we use [CI] as $C^0\ ^3P_1-^3P_0$) toward the W 3 GMC. The [CI] emission is widely extended over the molecular cloud, showing prominent peaks at W 3(Main), W 3(OH), and AFGL 333 clouds. This behavior is similar to that of the $^{12}CO\ J=1-0$ emission (Lada et al. 1978, Heyer et al. 1998). The [CI] distribution around the W 3(Main) and W 3(OH) clouds is consistent with that observed by Plume et al. (1999) and Kramer et al. (2004). We found that the [CI] intensity is strong in the AFGL 333 cloud. Weak [CI] emission extends to the west of the HDL, where no luminous IRAS source ($> 500 L_{\odot}$) is associated (Carpenter et al. 2000).

Fig. 2a shows the integrated intensity map of the [CI] line toward the AFGL 333 cloud. We found that the [CI] emission peak is about $100''$ offset to the west from the AFGL 333 HII region. Fig. 2b shows the integrated intensity map of the $C^{18}O\ J=1-0$ line. Intense $C^{18}O$ emission is detected along an filamentary-shaped ridge around the AFGL 333 HII region. Intense [CI] emission is detected toward this $C^{18}O$ ridge. We identified two molecular cores in the $C^{18}O$ ridge (A and B; Fig 2b). These cores are not associated with infrared sources nor radio continuum sources.

(b) The CCS, N_2H^+ , and $H^{13}CO^+$ Lines

We observe the CCS, N_2H^+ , and $H^{13}CO^+$ lines toward W 3 West: $(\alpha_{J2000}, \delta_{J2000}) = (2^h25^m30^s.4, 62^{\circ}05'51''.9)$, W 3(OH) A: $(\alpha_{J2000}, \delta_{J2000}) = (2^h27^m01^s.0, 61^{\circ}52'13''.9)$, AFGL 333 Core A: $(\alpha_{J2000}, \delta_{J2000}) = (2^h28^m6^s.1, 61^{\circ}29'27''.9)$, and AFGL 333 Core B: $(\alpha_{J2000}, \delta_{J2000}) = (2^h28^m03^s.2, 61^{\circ}27'45''.2)$. In the W 3(OH) region, we observed the position of IRAS 02232+6138,

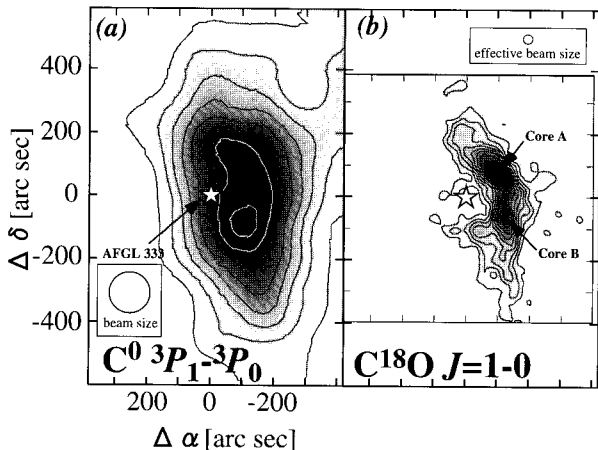


Fig. 2.— Integrated intensity maps of the C^0 $3P_1-3P_0$ emission and the $C^{18}O$ $J=1-0$ emission (b) toward the AFGL 333 cloud. The maps are centered on $(\alpha_{J2000}, \delta_{J2000}) = (2^h 28^m 21^s.5, 61^\circ 28' 29''.4)$.

which is $7''$ offset of the W 3(OH) UC HII region. This corresponds to the component (A) reported by Wilson et al. (1993). We call this position as W 3(OH) A.

The observed spectra are shown in Fig. 3. The $H^{13}CO^+$ intensities at all positions are similar. However the intensities of the N_2H^+ and CCS lines are different between the cores in the AFGL 333 cloud and other positions. Note that the CCS line is detected only in AFGL 333 Core A and Core B.

IV. DISCUSSION

(a) C^0 and CO

The CO and C^0 column densities are derived with the LTE assumption. A correlation diagram between $N(C^0)$ and $N(CO)$ is presented in Fig. 4. In this diagram, $N(C^0)$ linearly correlates with $N(CO)$ up to $N(CO) \sim 6 \times 10^{18} \text{ cm}^{-2}$, which corresponds to the visual extinction of 60 mag. The steady-state PDR models (e.g. Tielens & Hollenbach, 1985) predict that C^0 exists mainly in the region of $A_V < 10$, and $N(C^0)$ should be saturated around A_V of 10–20. Thus, the $N(C^0)$ - $N(CO)$ linear correlation up to $A_V \sim 60$ suggests an origin of C^0 unrelated to photodissociation processes. If the clouds have not reached at the chemical equilibrium, C^0 would be abundant in deep inside of molecular clouds. Since the averaged density of the clouds is $\sim 10^4 \text{ cm}^{-3}$, the conversion time scale from C^0 to CO is estimated to be 10^6 – 10^7 yr (Oka et al. 2004). The $N(C^0)$ - $N(CO)$ linear correlation may indicate that the clouds have formed within several times 10^6 yr.

In Fig. 4, $N(C^0)$ in the AFGL 333 cloud is higher than that in the W 3(OH) cloud in the same value of $N(CO)$, indicating that the $N(C^0)/N(CO)$ ratio of the AFGL 333 cloud is higher than that of the W 3(OH)

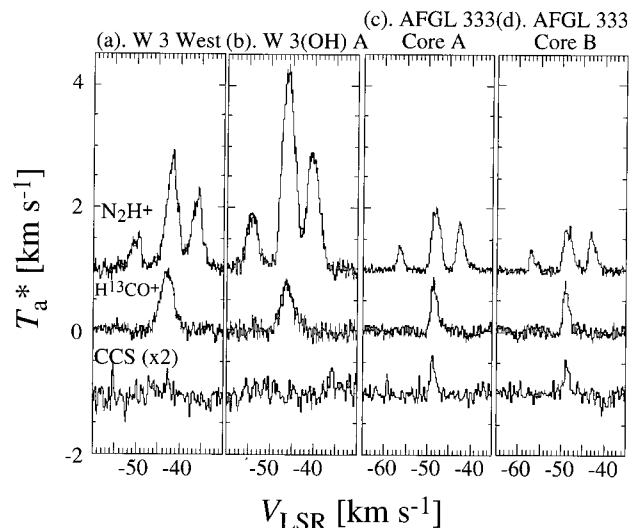


Fig. 3.— Spectra of the N_2H^+ , $H^{13}CO^+$, and CCS lines for W 3 West (a), W 3(OH) A (b), AFGL 333 Core A (c), AFGL 333 Core B (d).

cloud. This tendency may suggest that the AFGL 333 cloud is chemically younger than the W 3(OH) cloud.

(b) CCS and N_2H^+

Time-dependent model calculations predict that CCS is abundant in the early stage of chemical evolution and decreases with time within $\sim 10^6$ yr (e.g. Suzuki et al. 1992, Lee et al. 1996, Nejad & Wagenblast, 1999). This is because C^0 , which is abundant in early stage, plays an important role in production process of CCS. In contrast to CCS, the N_2H^+ and NH_3 abundances are high in the late stage. This is because these molecules are produced from N_2 , which is formed through neutral-neutral reactions (e.g. Nejad & Wagenblast, 1999). Thus it is thought that the CCS/N_2H^+ abundance ratio can be used as a chemical clock.

The column densities of N_2H^+ and CCS are derived with assuming the LTE condition. The $[CCS]/[N_2H^+]$ ratios in AFGL 333 Core A (0.4–0.9) and Core B (0.4–1.0) are found to be higher than those in W 3 West (< 0.2) and W 3(OH) A (< 0.06). The higher $[CCS]/[N_2H^+]$ ratio supports the notion that the AFGL 333 cloud is younger than the W 3(Main) and W 3(OH) clouds, as suggested by the $[C^0]/[CO]$ ratio.

(c) Dynamical Properties of the Clouds

We estimate the LTE and virial masses of the cores from the $C^{18}O$ data. The boundaries of the cores are determined with the CLUMPFIND algorithm (Williams et al. 1994). In the derivation of the LTE masses, the conversion factor from $N(C^{18}O)$ to $N(H_2)$ is employed to be 6×10^6 (Frerking et al. 1982). The virial mass of each core is calculated by the formula; $M_{VIR} = (5\Delta V^2 R) / (8G \ln(2))$. The LTE masses of Core

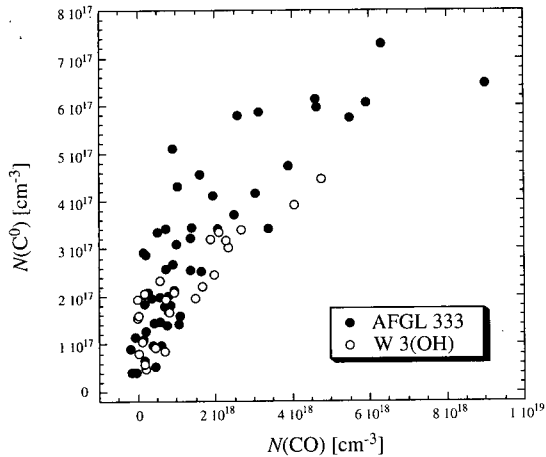


Fig. 4.— The C^0 column densities are plotted against the CO column densities.

A ($3.2 \times 10^3 M_{\odot}$) and Core B ($1.9 \times 10^3 M_{\odot}$) are similar to those of the cores in which massive stars are forming (Plume et al. 1997). The M_{VIR}/M_{LTE} ratio is calculated to be 0.3 and 0.3 for Core A and Core B, respectively, indicating that the cores are supercritical. Thus, it is most likely that active star formation will occur in there, and that the cores in the AFGL 333 cloud are in early stage of the massive star formation.

V. SUMMARY

We have revealed the [CI] distribution toward the almost whole region of the W 3 GMC. Then, we have found that the AFGL 333 cloud is chemically young, where the $[C^0]/[CO]$ and $[CCS]/[N_2H^+]$ ratios are high. In addition, two massive cores, which may be in early stage of massive star formation, are found in the AFGL 333 cloud.

ACKNOWLEDGEMENTS

The authors thank Gaku Saito for observing the C^0 $^3P_1-^3P_0$ line with the Mount Fuji Submillimeter Telescope. The authors are grateful to the NRO staff for excellent support in the 45 m observations. This study is supported by grants-in-aid from the Ministry of Education, Science, and Culture (07CE2002, 11304010, 12740119, and 10291056).

REFERENCES

- Carpenter, John M., Heyer, Mark H., Snell, & Ronald L., 2000, *ApJS*, 130, 381
- Frerking, M. A., Langer, W. D., & Wilson, R. W., 1982, *ApJ*, 262, 590
- Heyer, M. H., Brunt, C., Snell, R. L., Howe, J. E., Schloerb, F. P., & Carpenter, J. M., 1998, *ApJS*, 115, 241
- Hughes, V. A., & Viner, M. R. J., 1982, *AJ*, 87, 685
- Kramer, C., Jakob, H., Mookerjee, B., Schneider, N., Brüll, M., & Stutzki, J., 2004, *A&A*, 424, 887
- Kuboi, N., et al., 2005, *ApJ*, submitted
- Lada, C. J., Elmegreen, B. G., Cong, H.-I., & Thaddeus, P., 1978, *ApJL*, 226, L39
- Lee, H.-H., Herbst, E., Pineau des Forêts, G., Roueff, E., & Le Bourlot, J., 1996, *A&A*, 311, 690
- Massey, P., Johnson, K. E., & Degioia-Eastwood, K., 1995, *ApJ*, 454, 151
- Nejad, L. A. M., & Wagenblast, R., 1999, *A&A*, 350, 204
- Oka, T., Iwata, M., Maezawa, H., Ikeda, M., Ito, T., Kamegai, K., Sakai, T., & Yamamoto, S., 2004, *ApJ*, 602, 803
- Plume, R., Jaffe, D. T., Evans, Neal J., II; Martin-Pintado, J., & Gomez-Gonzalez, J., 1997, *ApJ*, 476, 730
- Plume, R., Jaffe, D. T., Tatematsu, K., Evans II, N. J., & Keene, J., 1999, *ApJ*, 512, 768
- Sakai T., Yamamoto, S., et al., 2005, in this issue
- Suzuki, H., Yamamoto, S., Ohishi, M., Kaifu, N., Ishikawa, S., Hirahara, Y., & Takano, S., 1992, *ApJ*, 392, 551
- Thronson, H. A., Jr., Campbell, M. F., & Hoffmann, W. F. I., 1980, *ApJL*, 229, L133
- Tieftrunk, A. R., Gaume, R. A., Claussen, M. J., Wilson, T. L., & Johnston, K. J., 1997, *A&A*, 239, 533
- Tieftrunk, A. R., Megeath, S. T., Wilson, T. L., & Rayner, J. T., 1998, *A&A*, 336, 991
- Tielens, A. G. G. M., & Hollenbach, D., 1985, *ApJ*, 291, 722
- Williams, J. P., de Geus, E. J., & Blitz, L., 1994, *ApJ*, 428, 693
- Wilson, T.L., Gaume, R.A., & Johnston, K.J., 1993, *ApJ*, 402, 230
- Yamamoto, S., & Saito, S., 1991, *ApJL*, 370, L103